Role of Diffusion-weighted MR Imaging in the Differentiation of Benign Retroperitoneal Fibrosis from Malignant Neoplasm: Preliminary Study[1]

Baris Bakir, MD
Fatma Yilmaz, MD
Rustu Turkay, MD
Sevda Özel, PhD
Bilge Bilgiç, MD
Arzu Velioglu, MD
Bulent Saka, MD
Artur Salmaslioglu, MD

Purpose: To evaluate diffusion-weighted imaging (DWI) features and signal intensity values at T2-weighted magnetic resonance (MR) imaging for differential diagnosis of benign retroperitoneal fibrosis (RPF) and plaque-like retroperitoneal malignant neoplasms.

Materials and Methods: Institutional review board approval and informed consent were obtained for this retrospective study. Fifty-one patients with plaque-like confluent retroperitoneal soft-tissue masses were divided into three groups: group I, 25 patients with malignant RPF and retroperitoneal malignant neoplasm; group II, 16 patients with chronic RPF; and group III, 10 patients with active RPF. On T1-weighted (unenhanced and contrast material–enhanced), T2-weighted, and DWI (b = 1000 sec/mm^2) images, apparent diffusion coefficient (ADC) values and quotients of postcontrast signal intensities between lesions and psoas muscle were evaluated. The χ^2 test was used to compare categorical values; one-way analysis of variance and Kruskal-Wallis tests were used to compare groups.

Results: Overall sensitivity, specificity, and positive and negative predictive values of DWI findings were 92% (23 of 25 patients), 62% (16 of 26 patients), 70% (23 of 33 patients), and 89% (16 of 18 patients), respectively. Mean ADC values were 0.79 ± 0.19 in group I, 1.43 ± 0.16 in group II, and 0.91 ± 0.14 in group III. When comparing values, differences between groups I and II (ADC values, $P < .0001$; DWI quotients, $P < .0001$; postcontrast quotients, $P = .001$) and groups II and III (ADC values, $P < .0001$; DWI quotients, $P = .016$; postcontrast quotients, $P = .04$) were significant. There was no significant difference between groups I and III or between the three groups when T2-weighted values were compared.

Conclusion: ADC of chronic RPF was higher than that for active RPF or malignant RPF and retroperitoneal malignant neoplasm. DWI can contribute to differential diagnosis of chronic RPF and malignant neoplasms with RPF morphology. Lesions in the malignant group and active RPF group had similar enhancement patterns, while those in the chronic RPF group demonstrated less enhancement. Signal intensity values on T2-weighted images were not useful for differentiating these conditions.

Online supplemental material is available for this article.

[1] From the Departments of Radiology (B. Bakir, F.Y., R.T., A.S.), Biostatistics and Medical Informatics (S.Ö.), Pathology (B. Bilgiç), and Internal Medicine (B.S.), Istanbul University, Istanbul Medical School, Capa, 34390 Istanbul, Turkey; and Department of Internal Medicine, Division of Nephrology, Marmara University Medical School, Istanbul, Turkey (A.V.). Received July 5, 2013; revision requested August 21; revision received November 28; accepted December 20; final version accepted February 7, 2014. **Address correspondence to** B. Bakir (e-mail: *drbarisbakir@yahoo.com*).

Retroperitoneal fibrosis (RPF) refers to a range of diseases characterized by the presence of a fibroinflammatory plaque-like confluent tissue that develops in the periaortic retroperitoneum (1,2). The abdominal aorta, iliac vessels, and, frequently, the inferior vena cava and ureters are surrounded by the tissue (1,3). Most often the disease is idiopathic; however, malignancy, surgery, drugs, or infections can be associated with this condition (1,4,5).

It has been reported that malignant cells are present in 8% of RPF cases (malignant RPF) (6). Also, malignant neoplasms in the para-aortacaval region (eg, lymphoma or malignant infiltration originating from the stomach, testis, kidney, pancreas, prostate, or endometrium) with plaque-like confluent tissue morphology (without fibrosis) may mimic RPF (7,8). It is important to differentiate benign RPF from malignant RPF and para-aortic malignant neoplasms to diagnose the underlying pathologic process and to determine the patient's prognosis. While dependent on the underlying cause, the prognosis for patients with benign RPF is generally favorable (4). On the other hand, the prognosis for malignant para-aortic neoplasm and malignant RPF is poor, with a mean survival of 3–6 months for malignant RPF (9–12).

Imaging findings—including the morphologic parameters of lesions, contrast material enhancement, and fluorine 18 fluorodeoxyglucose uptake patterns—and signal intensity characteristics on T2-weighted magnetic resonance (MR) images are used to differentiate benign RPF from malignant RPF (13–21). However, in two reviews that summarize these studies, it was reported that the imaging findings were not reliable enough to allow differentiation of benign RPF from malignant RPF (4,5).

While noninvasive imaging modalities can help exclude secondary causes of RPF, biopsy is often required for histologic confirmation, since imaging is ineffective in the differentiation of benign from malignant neoplasms. Biopsy results can yield a false-negative result, however, as metastatic cells may not have a homogeneous distribution in the fibrotic mass (4). Also, it is important to make the distinction between active and chronic (inactive) RPF for the therapeutic management of benign RPF cases (22).

The aim of this study was to evaluate the diffusion-weighted imaging (DWI) features and contribution of signal intensity values at T2-weighted MR imaging for the differential diagnosis of benign RPF and plaque-like retroperitoneal malignant neoplasms to determine whether DWI can be used to differentiate these entities.

Advances in Knowledge

- In patients with chronic retroperitoneal fibrosis (RPF), there was no restricted diffusion (16 [100%] of 16); however, in patients with active RPF (10 [100%] of 10), malignant RPF, and retroperitoneal malignant neoplasm with RPF morphology (23 [92%] of 25), there was restricted diffusion.
- When the apparent diffusion coefficient cutoff value was 1.05, the sensitivity and specificity in the differential diagnosis of chronic RPF versus malignant RPF and retroperitoneal malignant neoplasm were 96% and 100%, respectively (area under the receiver operating characteristic curve, 0.990; $P < .0001$).
- Signal intensity values on T2-weighted images were not useful in distinguishing these entities; there was no significant difference in T2-weighted values between the three groups ($P = .60$).

Implication for Patient Care

- Malignant lesions should be included in the differential diagnosis of para-aortocaval plaque-like lesions with RPF morphology if there is restricted diffusion on diffusion-weighted MR images.

Materials and Methods

Patients and Study Protocol

Institutional review board approval was obtained for this retrospective study, and informed consent was obtained from patients for participation in the research project. Between June 20, 2009, and September 1, 2012, 51 patients (mean age ± standard deviation, 57.06 years ± 10.85; range, 26–88 years) with plaque-like confluent retroperitoneal soft-tissue masses in the para-aortocaval region were included. Retroperitoneal isolated or multiple nodular masses or enlarged multiple lymph nodes constituted exclusion criteria. Forty of the 51 patients had various symptoms such as abdominal-lumbar pain, fatigue, weight loss, leg edema, and claudication. Patients were referred to our institution after a computed tomography and/or MR imaging examination performed in a different medical center demonstrated plaque-like confluent retroperitoneal soft-tissue masses in the para-aortocaval region. The remaining 11 patients had already received a diagnosis both clinically and

Published online before print
10.1148/radiol.14131565 **Content codes:** GU MR

Radiology 2014; 272:438–445

Abbreviations:
ADC = apparent diffusion coefficient
CI = confidence interval
DWI = diffusion-weighted imaging
ROI = region of interest
RPF = retroperitoneal fibrosis

Author contributions:
Guarantor of integrity of entire study, B. Bakir; study concepts/study design or data acquisition or data analysis/interpretation, all authors; manuscript drafting or manuscript revision for important intellectual content, all authors; approval of final version of submitted manuscript, all authors; literature research, B. Bakir, F.Y., R.T., B.S., A.S.; clinical studies, B. Bakir, F.Y., R.T., B. Bilgiç, A.V., B.S.; experimental studies, F.Y.; statistical analysis, B. Bakir, S.Ö.; and manuscript editing, B. Bakir, F.Y., B. Bilgiç, B.S., A.S.

Conflicts of interest are listed at the end of this article.

histopathologically, with chronic RPF at biopsy. Seventeen patients were women (mean age, 55.71 years ± 11.63; age range, 26–80 years), and 34 were men (mean age, 57.74 years ± 10.56; age range, 35–88 years). They were divided retrospectively into three groups on the basis of the final pathologic diagnosis. Group I included 25 patients with malignant RPF and retroperitoneal malignant neoplasm, group II included 16 patients with chronic RPF, and group III included 10 patients with active RPF. Details of inclusion and exclusion criteria are given in Appendix E1 (online).

MR Imaging Protocol

All imaging examinations were performed with a 1.5-T imaging system (Philips Achieva; Philips Medical Systems, Best, the Netherlands). MR images were obtained by using an eight-element phased-array multicoil for the body. The MR imaging study protocol consisted of a T1-weighted turbo spin-echo sequence, a T2-weighted turbo spin-echo sequence, and a multisection single-shot spin-echo echo-planar DWI sequence without breath holding (fat saturation was used to avoid chemical-shift artifacts). All sequences were performed in the axial planes. Also, in 25 of 51 patients (13 patients in group 1, six patients in group 2, and six patients in group 3), breath-hold T1-weighted fat-suppressed spoiled gradient-echo shared prepulse sequences were performed before contrast material administration and during the arterial, venous, and delayed phases after contrast material administration. The pulse sequence parameters are listed in Table 1.

Image Analysis

Images were evaluated by two observers in consensus on the day of the MR examination (B. Bakir, an abdominal radiologist, and F.Y., a general radiologist, with 10 and 5 years of MR experience, respectively) by using an Extended MR WorkSpace 2.6.3.5 workstation with Philips software.

For the qualitative analysis, the signal intensity of the lesions on DWI images (b = 1000 sec/mm^2) was evaluated visually. The lesion was considered hypointense if it had a signal intensity equal to or lower than that of the psoas muscles and hyperintense if it had a signal intensity higher than that of the psoas muscles. The signal intensity of the lesions on the ADC map was evaluated visually to determine if it was hypointense. The diffusion was considered restricted if a lesion had hyperintensity with a diffusion sequence (b = 1000 sec/mm^2) and hypointensity on apparent diffusion coefficient (ADC) maps.

Table 1

MR Imaging Parameters

Parameter	T1-weighted Turbo Spin Echo	T2-weighted Turbo Spin Echo	Multisection Single-Shot Spin-Echo DWI*	T1-weighted Fat-suppressed Spoiled Gradient Echo
Section thickness (mm)	6–8	6–8	6	4
Intersection gap	1.5–2	1.5–2	1	0.8
Repetition time (msec)	581	809	1812	5.11
Echo time (msec)	12	290	868	2.51
No. of signals acquired	1	1	3	1
Flip angle (degree)	90	90	90	10
Matrix size	308 × 305	216 × 216	256 × 256	352 × 352

* The b values were 0, 500, and 1000 sec/mm^2. The reduction factor and echo-planar imaging factor of the DWI sequence were 2 and 53, respectively.

Figure 1

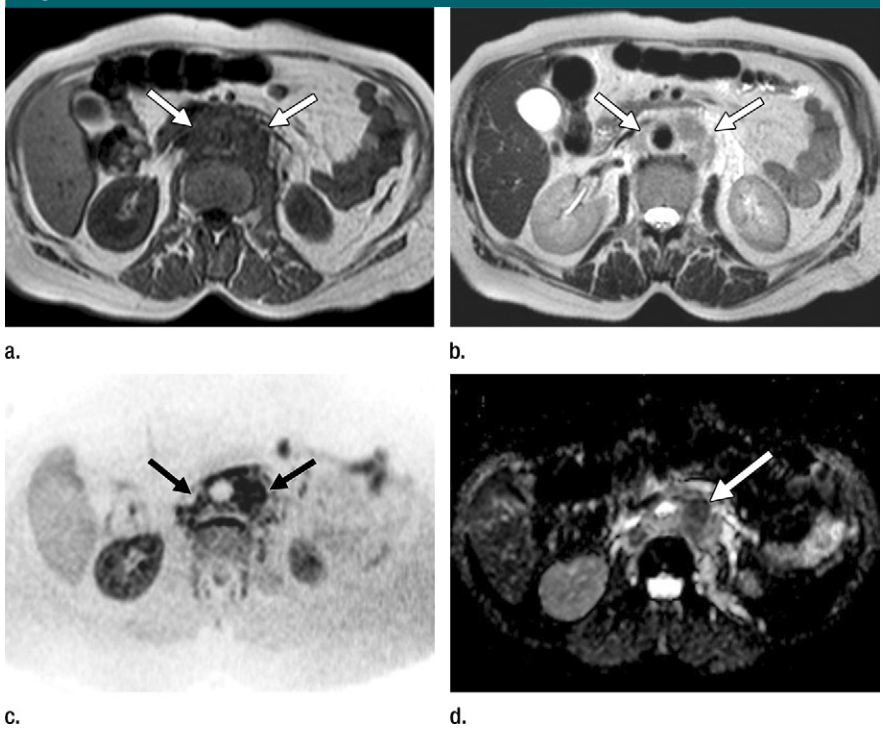

Figure 1: MR images in a 54-year-old man with malignant RPF (group I). **(a)** Axial T1-weighted and **(b)** axial T2-weighted MR images demonstrate plaque-like lesions at the para-aortocaval region surrounding the aorta (arrows). **(c)** DWI MR image (reverse image) demonstrates high signal intensity as dark areas in the lesion (arrows). **(d)** ADC map shows prominent hypointense areas in the lesion that correspond with low ADC values (arrow). Also see Figure E1 (online).

Figure 2

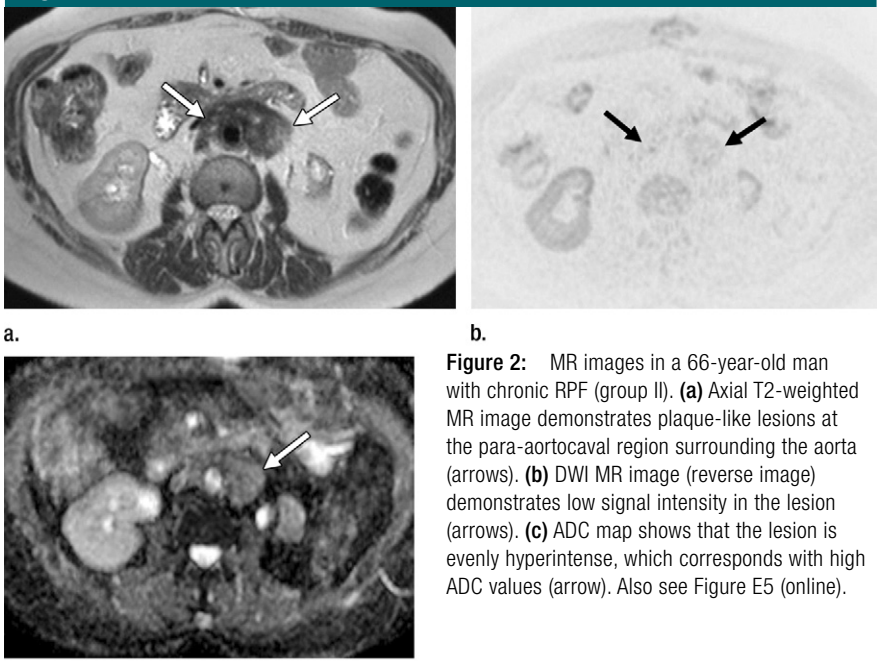

Figure 2: MR images in a 66-year-old man with chronic RPF (group II). **(a)** Axial T2-weighted MR image demonstrates plaque-like lesions at the para-aortocaval region surrounding the aorta (arrows). **(b)** DWI MR image (reverse image) demonstrates low signal intensity in the lesion (arrows). **(c)** ADC map shows that the lesion is evenly hyperintense, which corresponds with high ADC values (arrow). Also see Figure E5 (online).

For the quantitative analysis, one author (B. Bakir) placed regions of interest (ROIs) measuring at least 1 cm^2 (size range, 1–3.2 cm^2) on the lesions on DWI (b = 1000 sec/mm^2) and T2-weighted images, ADC maps, and postcontrast images (acquired in the delayed phases) by avoiding obvious areas of inhomogeneity. The ROI was placed within the lesions in the area with the lowest ADC value on ADC maps and areas with the highest signal intensity on DWI (b = 1000 sec/mm^2) and T2-weighted images. On postcontrast images, the ROI was placed in the areas with the most enhancement. At least three measurements were performed and averaged for each lesion. We used the same-size ROIs as those for the psoas lesions (B. Bakir placed all the ROIs).

For a comparative analysis of the DWI findings (b = 1000 sec/mm^2), signal intensity on T2-weighted images, and contrast enhancement patterns, we used a method similar to that reported by Arrive et al (9) and Kamper et al (23). We obtained quotients by dividing the mean signal intensity within the lesions by the intensity of the psoas muscle on the DWI (b = 1000 sec/mm^2), T2-weighted, and postcontrast images. We used the same sizes and positions of the ROI in the different sequences.

To compare pre- and posttreatment lesion sizes in the active RPF group, we measured the lesions' largest diameter at the para-aortocaval region.

Statistical Analyses

The sensitivity, specificity, and positive and negative predictive values of the DWI findings for the malignant (group I) and benign (groups II and III) groups were calculated with a 95% confidence interval (CI), according to qualitative signal intensity. The χ^2 test was used to compare sex within groups and the signal intensity of lesions on DWI images (b = 1000 sec/mm^2). To compare variables with a normal distribution (ADC, T2-weighted quotients) between three groups, the one-way analysis of variance test was used, and the Kruskal-Wallis test was used to compare variables without a normal distribution (DWI and postcontrast quotients). The Kolmogorov-Smirnov test with Lilliefors significance correction was used for the normality test.

We compared the malignant group (group I) with the chronic RPF group (group II) by using the following methods. The signal intensity of lesions on DWI images (b = 1000 sec/mm^2) was compared by using the χ^2 test. ADC values and DWI, T2-weighted, and postcontrast quotients were analyzed by using receiver operating characteristic curve analysis. The cutoff values for ADC values and DWI, T2-weighted, and postcontrast quotients were determined with receiver operating characteristic curve analysis. The correlation between ADC values and DWI and T2-weighted quotients was determined by using the Pearson correlation test.

The paired t test was used to compare pre- and posttreatment ADC values, DWI quotients, and lesion size in the active RPF group (group III). MedCalc (MedCalc Software, Mariakerke, Belgium) and IBM SPSS software, version 21.0 (IBM, Armonk, NY) were used. Significant differences were defined as $P < .05$.

Results

When the patient sex distribution was examined, the percentage of women in group I was 52% (13 of 25), and the percentage of men was 48% (12 of 25). In groups II and III, these values were 12% (two of 16) and 20% (two of 10) for women and 88% (14 of 16) and 80% (eight of 10) for men, respectively. While the patient sex distribution in group I was homogeneous, there was a male dominance in groups II and III (P = .02).

Comparison of Imaging Findings

On DWI images (b = 1000 sec/mm^2), 23 of the 25 patients in group I had a hyperintense lesion (Fig 1; Figs E1–E4 [online]), while two patients had hypointense lesions. (One of these patients received a diagnosis of mantle cell lymphoma, and the other received a diagnosis of adenocarcinoma infiltration from an unknown primary tumor. Both of these patients were untreated, and the lesions were sampled with core biopsy.) The lesions were hypointense in all patients in group II (Fig 2; Figs E5, E6 [online]) and hyperintense in

all patients in group III (Fig 3; Figs E7, E8 [online]). All of the hyperintense lesions on DWI images with *b* values of 1000 sec/mm^2 had low signal intensity (compatible with restricted diffusion) on ADC maps.

Mean ADC values and DWI, T2-weighted, and postcontrast quotients in the three groups are shown in Table 2. ADC values and DWI, T2-weighted, and postcontrast quotients of the groups are shown in Figures 4–7.

ADC values were different in each of the three groups ($P < .0001$). At post hoc analysis, the differences were significant between groups I and II and between groups II and III ($P < .0001$). However, there was no significant difference between groups I and III ($P = .154$).

When DWI quotients were compared, there was a difference between groups ($P < .0001$). At post hoc analysis, the differences were significant between groups I and II ($P < .0001$) and between groups II and III ($P = .016$). However, there was no significant difference between groups I and III ($P = .14$).

There was no significant difference in T2-weighted quotients between the three groups ($P = .60$).

When postcontrast quotients were compared, there was a difference between groups ($P = .001$). At post hoc analysis, the differences were significant between groups I and II ($P = .001$) and between groups II and III ($P = .04$). However, there was no significant difference between groups I and III ($P > .99$).

Comparison of Groups I and II

The qualitative difference of signal intensities on DWI images (b = 1000 sec/mm^2) between group I (3.72 ± 1.12) and group II (1.31 ± 0.39) was significant ($P < .0001$).

When the ADC cutoff value was 1.05, the sensitivity and specificity in the differential diagnosis of malignant neoplasia and chronic RPF were 96% and 100%, respectively (area under the receiver operating characteristic curve [AUC] = 0.990, Table 3). When the DWI quotient cutoff value was 1.99, the sensitivity and specificity were 92% and 100%, respectively (AUC = 0.975).

Figure 3

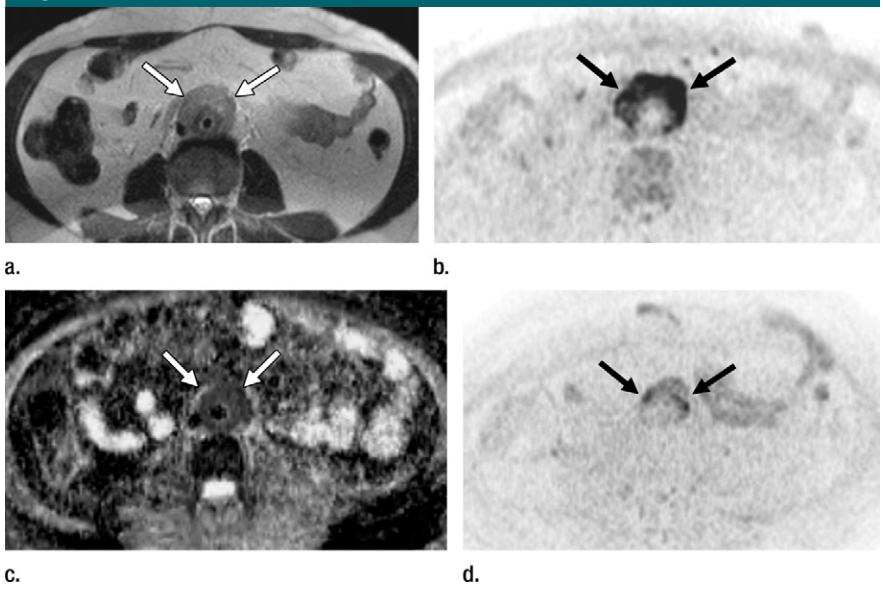

Figure 3: MR images in a 54-year-old man with acute inflammatory RPF (group III). **(a)** Axial T2-weighted MR image demonstrates plaque-like lesions at the para-aortocaval region surrounding the aorta (arrows). **(b)** DWI MR image (reverse image) demonstrates high signal intensity as dark areas in the lesion (arrows). **(c)** ADC map shows that the lesion is hypointense, which corresponds with low ADC values (arrows). **(d)** DWI MR image (reverse image) obtained 3 months after therapy demonstrates marked regression in the signal intensity of the lesion and a decrease in lesion size (arrows). Also see Figure E7 (online).

Table 2

Mean ADC Values and DWI, T2-weighted, and Postcontrast Quotients in Different Groups

Group	ADC*	DWI Quotient*	T2-weighted Quotient†	Postcontrast Quotient*
Group I (malignant)	0.79 ± 0.19	3.72 ± 1.12	2.37 ± 1.12	1.92 ± 0.15
Group II (chronic RPF)	1.43 ± 0.16	1.31 ± 0.39	2.17 ± 0.47	1 ± 0.12
Group III (active RPF)	0.91 ± 0.14	2.85 ± 0.40	2.25 ± 0.70	1.82 ± 0.14

Note.—Data are means ± standard deviations.

* Comparison yielded a significant difference ($P < .001$).

† Comparison did not yield a significant difference ($P = .605$).

When the T2-weighted quotient cutoff value was 2.65, the sensitivity was low (sensitivity, 40%; specificity, 87%; AUC = 0.552). When the postcontrast quotient cutoff value was 1.19, the sensitivity and specificity in the differential diagnosis of malignant neoplasia and chronic RPF were 100% and 100%, respectively (AUC = 1.000).

There was a significant reverse correlation between DWI quotient and ADC values ($r = -0.75$, $P < .0001$). There was no significant correlation between DWI and T2-weighted quotients ($r = 0.15$, $P = .349$) and between ADC values and T2-weighted quotients ($r = -0.16$, $P = .301$).

When all of the patients were included in the evaluation, the sensitivity, specificity, positive predictive value, and negative predictive value of DWI MR sequences in the differential diagnosis of malignant and benign lesions were 92% (95% CI: 74%, 99%), 62%

Figure 4

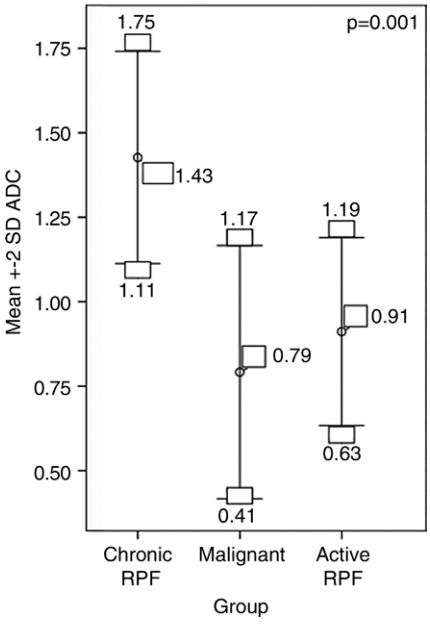

Figure 4: Graph shows the distribution of ADC values in three groups. (Values are means ± standard deviation [*SD*].)

Figure 5

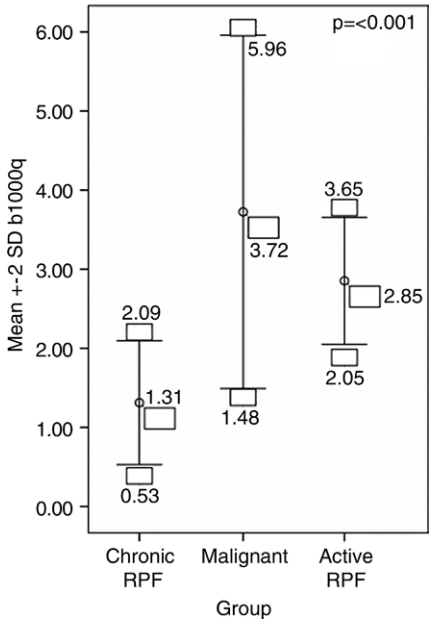

Figure 5: Graph shows the distribution of DWI (*b* = 1000 sec/mm^2) values *(b1000q)* in three groups. (Values are means ± standard deviation [*SD*].)

Figure 6

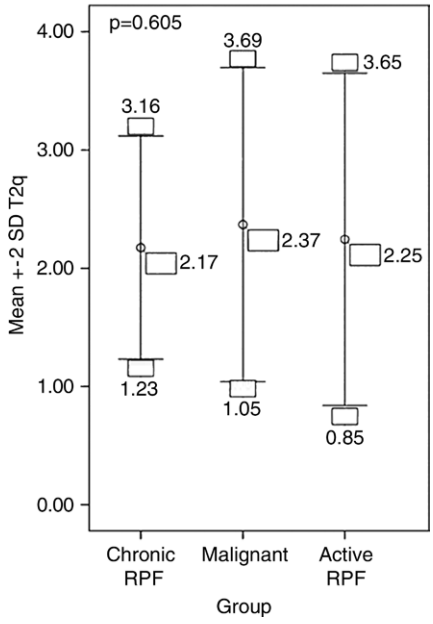

Figure 6: Graph shows the distribution of T2-weighted *(T2q)* values in the three groups. (Values are means ± standard deviations [*SD*].)

Figure 7

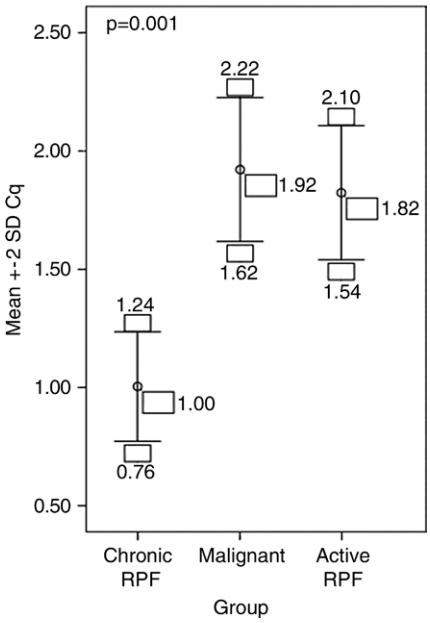

Figure 7: Graph shows the distribution of postcontrast *(Cq)* values in the three groups. (Values are means ± standard deviation [*SD*].)

Table 3

Cutoff Points and AUCs for ADC Values and DWI, T2-weighted, and Postcontrast Quotient Variables in the Differential Diagnosis of Group I (Malignant Group) and Group II (Chronic RPF Group)

Parameter	Cutoff Point	Sensitivity (%)	95% CI for Sensitivity	Specificity (%)	95% CI for Specificity	AUC
DWI quotient	>1.99	92	74.0, 99.0	100	79.4, 100.0	0.975
ADC	≤1.05	96	79.6, 99.9	100	79.4, 100.0	0.990
T2-weighted quotient	>2.61	40	21.1, 61.3	87	61.7, 98.4	0.552
Postcontrast quotient	>1.19	100	75.3, 100.0	100	54.1, 100.0	1.000

(95% CI: 41%, 80%), 70% (95% CI: 51%, 84%), and 89% (95% CI: 65%, 99%), respectively.

In eight patients in group I who underwent a control MR imaging examination and a follow-up MR imaging examination, the mean pretreatment DWI quotients and ADC values were 2.86 ± 0.38 and 0.91 ± 0.14, respectively; posttreatment mean DWI quotient was 1.21 ± 0.21, and ADC value was 1.44 ± 0.16 ($P < .001$).

In the follow-up MR examination of the eight patients (posttreatment), there was also regression on the lesion size at the para-aortacaval region (while pretreatment mean lesion diameter was 17.25 mm ± 4.46 and posttreatment mean lesion diameter was 7.25 mm ± 3.20 [$P < .001$]).

Discussion

We detected restricted diffusion on DWI images in 23 (92%) of 25 patients in the malignant group, 10 of 10 in the active RPF group, and 0 of 16 in the chronic RPF group. The reason why acute RPF demonstrated restricted diffusion while chronic RPF did not

might be related to the different time of onset of the processes. In the early stages of fibrosis, highly vascular tissue and collagen are present in the plaque, in addition to polyclonal B and CD4+ T cell infiltrates, plasma cells, histiocytes, and macrophages. Later, fibrosis replaces inflammatory tissue (5). In the early stages where the cellular content of the plaque is high, water diffusion may be restricted, owing to the reduced extracellular space and also to cell membranes acting like a barrier to water movement. In the chronic stage, with the regression of the inflammation and the onset of fibrosis, the less cellular environment and the relative increase in extracellular stage allow freer water diffusion. The restricted diffusion in the malignant group, like active RPF, might be due to their highly cellular environment. In our study, however, two patients with malignant RPF demonstrated no restricted diffusion. Arrive et al suggested that instead of using morphologic features and enhancement patterns at MR imaging, signal intensity characteristics on T2-weighted images (by using a technique similar to ours with comparison of signal intensity on T2-weighted images between the lesion and muscle) are more useful in differentiating benign and malignant RPF (9). In our study, however, there was no significant signal intensity difference on T2-weighted images between benign and malignant RPF. The reason for these differing results is not clear. In addition, while the number of examinations with contrast material administration in our study was low (n = 25), we have observed that the lesions in the malignant group and active RPF group had similar enhancement patterns, while the lesions in the chronic RPF group demonstrated less enhancement compared with the others.

Other authors have assessed the role of DWI in the differential diagnosis of retroperitoneal masses and RPF. In the study by Rosenkrantz et al, which included 22 patients with RPF and nine patients with lymphoma, the ADC was significantly lower in lymphoma than in RPF (mean, $[0.92 \pm 0.17] \times 10^{-3}$ mm^2/sec vs $[1.40 \pm 0.38] \times 10^{-3}$ mm^2/sec; P = .003) (7). However, in a study by Spieler et al, which included 11 RPF and 16 lymphoma cases, there was no significant difference in mean ADC values between lymphoma (1.26×10^{-3} mm^2/sec; range, $[0.54–2.03] \times 10^{-3}$ mm^2/sec) and RPF (1.35×10^{-3} mm^2/sec; range, $[0.61–2.45] \times 10^{-3}$ mm^2/sec) (P = .57) (24). The discrepancies between these two studies may be due to the fact that neither of them had made a distinction between active and chronic RPF. Furthermore, the different selection criteria for the malignant case groups might have created this discrepancy. For example, two cases in our study (a lymphoma and an adenocarcinoma) did not exhibit restricted diffusion, thereby mimicking the chronic RPF group.

Another observation in our study was the absence of restricted diffusion at follow-up MR imaging in all eight patients treated for acute RPF. Also, ADC values in eight patients were increased compared with pretreatment ADC values. The mean pretreatment ADC value in the eight patients was 0.91 ± 0.14, which increased to 1.44 ± 0.16 3–6 months after treatment. This can be explained by the posttreatment decrease in cell population density in acute RPF and the more pronounced fibrosis.

Our study had limitations. Our patient population size was limited. This was especially true for the acute RPF group, where some statistical analyses could not be performed owing to small sample size. In addition, the number of patients evaluated for contrast enhancement was low in all groups. Another limitation was that only core biopsy was used for lesion sampling in most cases, which prevented a precise radiopathologic correlation. A further shortcoming of our study was that we did not assess the reproducibility of quantitative DWI measurements. Also, ADC values can demonstrate variation, depending on the choice of b values used. The ADC cutoff values in our study were determined by using retrospective evaluation. These findings need to be validated in separate, prospectively acquired data sets.

In conclusion, the ADC value of chronic RPF is statistically higher than that for acute RPF or malignant RPF and retroperitoneal malignant neoplasia with an RPF morphology. We observed that if restricted diffusion was detected in a para-aortic plaque-like mass, the differential diagnosis included a malignant neoplasm (including malignant RPF) or active RPF; if there was no restricted diffusion, however, the differential diagnosis included chronic RPF. A biopsy would still be required for differentiation of active from malignant RPF, but DWI might also be useful during biopsy procedures in targeting presumptive tumoral nests in plaque lesions and in the evaluation of treatment in acute RPF cases. Additional studies with larger patient populations could better clarify the contribution of DWI in the diagnosis of disease and treatment of patients.

Disclosures of Conflicts of Interest: B. Bakir No relevant conflicts of interest to disclose. **F.Y.** No relevant conflicts of interest to disclose. **R.T.** No relevant conflicts of interest to disclose. **S.Ö.** No relevant conflicts of interest to disclose. **B. Bilgiç** No relevant conflicts of interest to disclose. **A.V.** No relevant conflicts of interest to disclose. **B.S.** No relevant conflicts of interest to disclose. **A.S.** No relevant conflicts of interest to disclose.

References

1. Vaglio A, Salvarani C, Buzio C. Retroperitoneal fibrosis. Lancet 2006;367(9506):241–251.
2. Palmisano A, Vaglio A. Chronic periaortitis: a fibro-inflammatory disorder. Best Pract Res Clin Rheumatol 2009;23(3):339–353.
3. Fritz J, Horger M, Wehrmann M. Computer tomography of retroperitoneal fibrosis [in German]. Rofo 2006;178(5):463–467.
4. Cronin CG, Lohan DG, Blake MA, Roche C, McCarthy P, Murphy JM. Retroperitoneal fibrosis: a review of clinical features and imaging findings. AJR Am J Roentgenol 2008; 191(2):423–431.
5. Monev S. Idiopathic retroperitoneal fibrosis: prompt diagnosis preserves organ function. Cleve Clin J Med 2002;69(2):160–166.
6. Lepor H, Walsh PC. Idiopathic retroperitoneal fibrosis. J Urol 1979;122(1):1–6.
7. Rosenkrantz AB, Spieler B, Seuss CR, Stifelman MD, Kim S. Utility of MRI features for

differentiation of retroperitoneal fibrosis and lymphoma. AJR Am J Roentgenol 2012; 199(1):118–126.

8. Heckmann M, Uder M, Kuefner MA, Heinrich MC. Ormond's disease or secondary retroperitoneal fibrosis? An overview of retroperitoneal fibrosis. Rofo 2009;181(4): 317–323.
9. Arrivé L, Hricak H, Tavares NJ, Miller TR. Malignant versus nonmalignant retroperitoneal fibrosis: differentiation with MR imaging. Radiology 1989;172(1):139–143.
10. Koep L, Zuidema GD. The clinical significance of retroperitoneal fibrosis. Surgery 1977; 81(3):250–257.
11. Vivas I, Nicolás AI, Velázquez P, Elduayen B, Fernández-Villa T, Martínez-Cuesta A. Retroperitoneal fibrosis: typical and atypical manifestations. Br J Radiol 2000;73(866): 214–222.
12. Lalli AF. Retroperitoneal fibrosis and inapparent obstructive uropathy. Radiology 1977; 122(2):339–342.
13. Rubenstein WA, Gray G, Auh YH, et al. CT of fibrous tissues and tumors with sonographic correlation. AJR Am J Roentgenol 1986; 147(5):1067–1074.
14. Brun B, Laursen K, Sørensen IN, Lorentzen JE, Kristensen JK. CT in retroperitoneal fibrosis. AJR Am J Roentgenol 1981;137(3): 535–538.
15. Amis ES Jr. Retroperitoneal fibrosis. AJR Am J Roentgenol 1991;157(2):321–329.
16. Mulligan SA, Holley HC, Koehler RE, et al. CT and MR imaging in the evaluation of retroperitoneal fibrosis. J Comput Assist Tomogr 1989;13(2):277–281.
17. Brooks AP. Computed tomography of idiopathic retroperitoneal fibrosis ('periaortitis'): variants, variations, patterns and pitfalls. Clin Radiol 1990;42(2):75–79.
18. Degesys GE, Dunnick NR, Silverman PM, Cohan RH, Illescas FF, Castagno A. Retroperitoneal fibrosis: use of CT in distinguishing among possible causes. AJR Am J Roentgenol 1986;146(1):57–60.
19. Fagan CJ, Larrieu AJ, Amparo EG. Retroperitoneal fibrosis: ultrasound and CT features. AJR Am J Roentgenol 1979;133(2):239–243.
20. Chander S, Ergun EL, Chugani HT, et al. High 2-deoxy-2-[18F]fluoro-D-glucose accumulation in a case of retroperitoneal fibrosis following resection of carcinoid tumor. Mol Imaging Biol 2002;4(5):363–368.
21. Mirault T, Lambert M, Puech P, et al. Malignant retroperitoneal fibrosis: MRI characteristics in 50 patients. Medicine (Baltimore) 2012;91(5):242–250.
22. Alberti C. Retroperitoneal fibroses: aetiopathogenesis and taxonomic assessment. Eur Rev Med Pharmacol Sci 2007;11(6):375–382.
23. Kamper L, Brandt AS, Scharwächter C, et al. MR evaluation of retroperitoneal fibrosis. Rofo 2011;183(8):721–726.
24. Spieler B, Reuben Seuss C, Sahlein D, Kim S. Diffusion-weighted imaging of retroperitoneal fibrosis and retroperitoneal lymphoma: can apparent diffusion coefficient values distinguish the two? [abstr]. In: Proceedings of the Nineteenth Meeting of the International Society for Magnetic Resonance in Medicine. Berkeley, Calif: International Society for Magnetic Resonance in Medicine, 2011; 2981.